

## Quantitative Physiology of Non-Energy-Limited Retentostat Cultures of *Saccharomyces cerevisiae* at Near-Zero Specific Growth Rates

Liu, Yaya; El Masoudi, Anissa; Pronk, Jack T.; van Gulik, Walter M.

**DOI**

[10.1128/AEM.01161-19](https://doi.org/10.1128/AEM.01161-19)

**Publication date**

2019

**Document Version**

Accepted author manuscript

**Published in**

Applied and Environmental Microbiology

**Citation (APA)**

Liu, Y., El Masoudi, A., Pronk, J. T., & van Gulik, W. M. (2019). Quantitative Physiology of Non-Energy-Limited Retentostat Cultures of *Saccharomyces cerevisiae* at Near-Zero Specific Growth Rates. *Applied and Environmental Microbiology*, 85(20), Article e01161-19. <https://doi.org/10.1128/AEM.01161-19>

**Important note**

To cite this publication, please use the final published version (if applicable). Please check the document version above.

**Copyright**

Other than for strictly personal use, it is not permitted to download, forward or distribute the text or part of it, without the consent of the author(s) and/or copyright holder(s), unless the work is under an open content license such as Creative Commons.

**Takedown policy**

Please contact us and provide details if you believe this document breaches copyrights. We will remove access to the work immediately and investigate your claim.

1 **Quantitative physiology of non-energy-limited retentostat cultures of *Saccharomyces***  
2 ***cerevisiae* at near-zero specific growth rates**

3 Yaya Liu, Anissa el Masoudi<sup>a</sup>, Jack T. Pronk, Walter M. van Gulik<sup>#</sup>

4

5 Department of Biotechnology, Delft University of Technology, Van der Maasweg 9, 2629 HZ  
6 Delft, The Netherlands

7

8 <sup>#</sup> Corresponding author: W.M. van Gulik, e-mail [w.m.vangulik@tudelft.nl](mailto:w.m.vangulik@tudelft.nl), telephone

9 +31152784629

10

11 **Key words:** yeast physiology, near-zero growth, retentostat, non-energy limitation, carbon

12 excess

13

14

15

16

17

18

19

20

21

---

<sup>a</sup> Current address: Royal Haskoning DHV, George Hintzenweg 85, 3009 AM Rotterdam, The Netherlands.

22 **Abstract:**

23 So far, the physiology of *Saccharomyces cerevisiae* at near-zero growth rates has been  
24 studied in retentostat cultures with a growth-limiting supply of the carbon and energy  
25 source. Despite its relevance in nature and industry, the near-zero growth physiology of *S.*  
26 *cerevisiae* under conditions where growth is limited by the supply of non-energy substrates  
27 remains largely unexplored. This study analyses the physiology of *S. cerevisiae* in aerobic  
28 chemostat and retentostat cultures grown under either ammonium or phosphate limitation.  
29 To compensate for loss of extracellular nitrogen- or phosphorus-containing compounds,  
30 establishing near-zero growth rates ( $\mu < 0.002 \text{ h}^{-1}$ ) in these retentostats required addition of  
31 low concentrations of ammonium or phosphate to reservoir media. In chemostats as well as  
32 in retentostats, strongly reduced cellular contents of the growth-limiting element (nitrogen  
33 or phosphorus) and high accumulation levels of storage carbohydrates were observed. Even  
34 at near-zero growth rates, culture viability in non-energy-limited retentostats remained  
35 above 80 % and ATP synthesis was still sufficient to maintain an adequate energy status and  
36 keep cells in a metabolic active state. Compared to similar glucose-limited retentostat  
37 cultures, the nitrogen- and phosphate-limited cultures showed a partial uncoupling of  
38 catabolism and anabolism and aerobic fermentation. The possibility to achieve stable, near-  
39 zero growth cultures of *S. cerevisiae* under nitrogen- or phosphorus-limitation offers  
40 interesting prospects for high-yield production of bio-based chemicals.

41 **Importance:**

42 The yeast *Saccharomyces cerevisiae* is a commonly used microbial host for production of  
43 various bio-chemical compounds. From a physiological perspective, biosynthesis of these  
44 compounds competes with biomass formation in terms of carbon and/or energy equivalents.  
45 Fermentation processes functioning at extremely low or near-zero growth rates would

46 prevent loss of feedstock to biomass production. Establishing *S. cerevisiae* cultures in which  
47 growth is restricted by the limited supply of a non-energy substrate could therefore have a  
48 wide range of industrial applications, but remains largely unexplored. In this work we  
49 accomplished near-zero growth of *S. cerevisiae* through limited supply of a non-energy  
50 nutrient, namely the nitrogen or phosphorus source and carried out a quantitative  
51 physiology study of the cells under these conditions. The possibility to achieve near-zero-  
52 growth *S. cerevisiae* cultures through limited supply of a non-energy nutrient may offer  
53 interesting prospects to develop novel fermentation processes for high-yield production of  
54 bio-based chemicals.

## 55 **Introduction**

56 The yeast *Saccharomyces cerevisiae* is an established microbial host for production of a wide  
57 range of bio-chemical compounds (1, 2). Current aerobic processes for production of ATP-  
58 requiring ('anabolic') products are typically biphasic, with separate growth and production  
59 phases. Complete uncoupling of growth and product formation could enable a further  
60 reduction of the loss of feedstock to biomass production. In theory, such a complete  
61 uncoupling can be achieved in continuous processes performed at very low or near-zero  
62 specific growth rates. In practice, however, its implementation requires processes and  
63 microorganisms that, over prolonged periods of time, ensure a high viability and a high  
64 biomass-specific product formation rate ( $q_p$ ) in the absence of growth.

65 For laboratory studies near-zero specific growth rates are usually achieved in retentostats (3).

66 A retentostat is a modification of the chemostat, in which effluent removal occurs through  
67 an internal or external filter module that causes complete biomass retention. Retentostats  
68 enable studies on microbial physiology at near-zero growth rates that are technically difficult

69 to achieve in conventional chemostats, while their use avoids complete starvation by  
70 maintaining a constant supply of essential nutrients.

71 When growth in retentostat cultures is limited by the energy substrate, biomass  
72 accumulates in the reactor until the biomass-specific substrate consumption rate ( $q_s$ ) equals  
73 the energy-substrate requirement for cellular maintenance ( $m_s$ ). Aerobic and anaerobic,  
74 glucose-limited retentostat cultures of *S. cerevisiae* were shown to retain a high viability, as  
75 well as an extremely high heat-shock tolerance, over periods of several weeks (4-7).

76 Consistent with a growth-rate-independent requirement of ATP for cellular maintenance (8),  
77 observed values of  $q_s$  at near-zero growth rates ( $\mu < 0.002 \text{ h}^{-1}$ ) were in good agreement with  
78 estimates of  $m_s$  derived from measurements in glucose-limited chemostat cultures grown at  
79 a range of specific growth rates (4, 6).

80 From an applied perspective, it seems illogical to apply severely energy-limited cultivation  
81 regimes for production of compounds whose synthesis from sugar requires a net input of  
82 ATP. In nature, *S. cerevisiae* seems to have primarily evolved for growth in sugar-rich  
83 environments where, instead of the energy substrate, the nitrogen source is growth limiting  
84 (9, 10). Also in industrial substrates for *S. cerevisiae* such as wine most or brewing wort,  
85 sugar is typically present in abundance, while growth becomes limited by the nitrogen  
86 source (11). As an alternative to nitrogen-limited cultivation, growth under extreme  
87 phosphate limitation may offer interesting options to uncouple growth from product  
88 formation. For example, *S. cerevisiae*, a non-oleaginous yeast, has been reported to  
89 accumulate high levels of specific fatty acids when availability of phosphate is restricted (12).

90 Studies in exponentially growing chemostat cultures have revealed an extensive  
91 reprogramming of the yeast transcriptome, proteome and fluxome in response to nitrogen  
92 and phosphorus limitation (13-16). In addition, nitrogen- and phosphorus-limited growth of

93 resulted in lower contents of protein and phospholipids, respectively, in yeast biomass (17,  
94 18). In contrast to the wealth of data on the effects of different nutrient limitation regimes in  
95 actively growing cultures, information on aerobic *S. cerevisiae* cultures grown at near-zero  
96 growth rates is scarce. In anaerobic cultures, nitrogen-limited cultivation with biomass  
97 recycling has been explored to maximize ethanol yields (19, 20). Brandberg and coauthors  
98 (21), who investigated the impact of severe nitrogen limitation on ethanol production by *S.*  
99 *cerevisiae*, used incomplete cell recycling under anaerobic and micro-aerobic conditions.  
100 The goal of the present study is to design and implement retentostat regimes for aerobic,  
101 nitrogen- and phosphate-limited growth of *S. cerevisiae* at near-zero specific growth rates  
102 and to use the resulting cultures for a first experimental exploration of its quantitative  
103 physiology under these scientifically interesting and industrially relevant conditions. To this  
104 end, experimental setups were tested that allowed for a smooth transition from low growth  
105 rate chemostat cultures to near-zero growth rate retentostat cultures. Metabolic fluxes,  
106 biomass composition and cellular robustness were analysed and compared with previously  
107 obtained data from glucose-limited chemostat and retentostat cultures.

## 108 **Results**

### 109 **Design of carbon-excess retentostat regimes**

110 To study the physiology of *S. cerevisiae* at near-zero growth rates under non-energy-limited  
111 conditions, retentostat regimes were designed in which growth was prevented by a severely  
112 limited supply of ammonium or phosphate. To avoid starvation, any loss of nitrogen or  
113 phosphate from such cultures, either by cell lysis or by excretion of N- or P-containing  
114 compounds from viable cells, should be compensated for. As a first approximation of the  
115 rates of N and P release by *S. cerevisiae* at near-zero growth rates, concentrations of N- and

116 P-containing compounds were quantified in the outflow of an aerobic, glucose-limited  
117 retentostat culture. From these measurements, biomass-specific release rates of 8.1  $\mu\text{mol}$   
118  $\text{N}/[\text{g biomass}]/\text{h}$  and 5.2  $\mu\text{mol P}/[\text{g biomass}]/\text{h}$  were calculated (Supplementary Table S1).  
119 These rates were used to estimate required supply rates of ammonium and phosphate in  
120 non-growing retentostat cultures limited by either of these two nutrients. For a target  
121 biomass concentration in the retentostats of 5 g/L at a dilution rate of  $0.025 \text{ h}^{-1}$ , 0.1 g/L  
122  $(\text{NH}_4)_2\text{SO}_4$  was included in the medium feed of the ammonium-limited cultures, while 0.014  
123 g/L  $\text{KH}_2\text{PO}_4$  was used for phosphate-limited retentostat cultivation.

124 Aerobic growth of *S. cerevisiae* at non-limiting concentrations of glucose leads to aerobic  
125 alcoholic fermentation (22). Based on trial experiments, glucose concentrations in the  
126 influent of ammonium- and phosphate-limited retentostats were set at 120 g/L and 60 g/L,  
127 respectively. These concentrations of the growth-limiting nutrients resulted in residual  
128 glucose concentrations of ca. 15 g/L. Ethanol concentrations did not exceed 20 g/L, which is  
129 well below the value of 5 % (v/v) that has been reported to cause stress responses (23).

### 130 **Growth and viability in ammonium- and phosphate-limited retentostat cultures**

131 Retentostat cultures were started by redirecting the effluent of steady-state ammonium- or  
132 phosphate-limited chemostat cultures, grown at a dilution rate of  $0.025 \text{ h}^{-1}$ , through a  
133 membrane filter unit placed inside the reactor (see Materials and Methods). Replicate  
134 ammonium-limited retentostats were operated for 220 h with full biomass retention, after  
135 which fouling caused the membrane filters to clog. Membrane fouling was not observed in  
136 the phosphate-limited retentostats, which were operated with full biomass retention until,  
137 after 400 h, the biomass concentration had reached a stable value.

138 Irrespective of the nutrient limitation regime, the onset of retentostat cultivation led to a  
139 gradual increase of the biomass concentration (Fig. 1A and 1B). In ammonium-limited  
140 retentostats, the biomass concentration stabilized at ca. 14 g/L after 150 h, while  
141 stabilization in the phosphate-limited cultures at ca. 18 g/L occurred after 300 h. The  
142 increase in biomass concentration in the ammonium-limited retentostats mainly reflected an  
143 increase of the dry mass per cell, which was initially smaller than in the phosphate-limited  
144 retentostats. Conversely, the biomass increase in phosphate-limited retentostats  
145 predominantly reflected an increase of the cell number (Fig. 1C and 1D).

146 Culture viability was estimated by plate counts of colony-forming units (CFU) and by flow  
147 cytometry after CFDA/propidium iodide (PI) staining (Supplementary Table S2). We observed  
148 a consistently lower viability in the CFU assays than in the CFDA/PI stains. A similar  
149 difference has previously been attributed to loss of viability of retentostat-grown cells during  
150 plating (4, 6). Based on PI staining, the viability of the ammonium- and phosphate-limited  
151 retentostat cultures towards the end of the experiments did not decrease below 80 % and  
152 90 %, respectively (Fig. 1A and 1B, Supplementary Table S2).

153 During retentostat cultivation, specific growth rates progressively decreased, reaching final  
154 values of  $0.00056 \pm 0.00010 \text{ h}^{-1}$  and  $0.00043 \pm 0.00012 \text{ h}^{-1}$  for the ammonium- and  
155 phosphate-limited cultures, respectively, corresponding to doubling times of 55 and 67 days  
156 (Fig. 1E and 1F). Based on these observations, death rates of  $0.0018 \pm 0.0001 \text{ h}^{-1}$  and  $0.0012$   
157  $\pm 0.0001 \text{ h}^{-1}$  were calculated for prolonged ammonium- and phosphate-limited retentostat  
158 cultures, respectively. The resulting gradual decrease of culture viability partially explained  
159 the difference between the observed biomass accumulation and the targeted values in the  
160 experimental design.

## 161 **Quantitative physiology under extreme ammonium and phosphate limitation**

162 During retentostat cultivation, the biomass-specific consumption rates of glucose and  
163 oxygen and production rates of ethanol and CO<sub>2</sub> asymptotically decreased over time and  
164 stabilized after approximately 100 h in the ammonium-limited cultures and after  
165 approximately 200 h in the phosphate-limited cultures (Supplementary Fig. S1). At this stage,  
166 the specific growth rate of the cultures was lower than 0.002 h<sup>-1</sup>, growth stoichiometries  
167 became constant (Fig. 1E and 1F) and cells were assumed to be in a metabolic pseudo steady  
168 state. Physiological parameters obtained from the preceding, slowly growing steady-state  
169 chemostat cultures ( $\mu = 0.025 \text{ h}^{-1}$ ) and from the pseudo-steady-state, near-zero growth  
170 retentostat cultures ( $\mu < 0.002 \text{ h}^{-1}$ ) are summarized in Table 1. As anticipated, the  
171 concentrations of the limiting nutrients (ammonium or phosphate) were below the  
172 detection limit, whereas glucose concentrations were between 10 and 20 g/L in all cultures  
173 (Table 1). Carbon- and degree-of-reduction balances yielded recoveries close to 100 % (Table  
174 1), indicating that no major metabolites had been overlooked in the analyses.

175 In the slow-growing ( $\mu = 0.025 \text{ h}^{-1}$ ) chemostat cultures the biomass-specific rates of glucose  
176 and oxygen consumption as well as ethanol and carbon dioxide production, were  
177 consistently higher in the phosphate-limited cultures than in the ammonium-limited cultures  
178 (Table 1). In line with these observations, the phosphate-limited cultures showed a lower  
179 biomass yield and higher ethanol yield on glucose. Respiratory quotients (RQ, ratio of CO<sub>2</sub>  
180 production and O<sub>2</sub> consumption rate) were identical for the two nutrient limitation regimes,  
181 indicating that the difference in biomass yield of the chemostat cultures was not caused by  
182 different contributions of respiratory and fermentative metabolism. Furthermore, the sum  
183 of the specific production rates of the four minor byproducts (glycerol, succinate, lactate and  
184 acetate), which accounted for less than 4 % of the consumed glucose, were not significantly

185 different for the two limitation regimes and were also not responsible for the observed  
186 difference in biomass yield.

187 In the pseudo-steady-state near-zero growth retentostat cultures, the observed ethanol  
188 yields on glucose (Table1) were respectively 71 % and 53 % of the theoretical maximum  
189 (0.51 g ethanol/[g glucose]) for the ammonium- and phosphate-limited regimes. Consistent  
190 with this observation, significant oxygen consumption occurred in these cultures and their  
191 RQ values were significantly lower than those of the preceding chemostat cultures. For the  
192 phosphate-limited cultures the difference was most pronounced. These observations  
193 indicate that near-zero growth achieved by phosphate limitation leads to a more respiratory  
194 metabolism than was observed in the preceding slowly growing, phosphate-limited  
195 chemostats. Formation of byproducts accounted for 16 % and 11 % of the supplied glucose  
196 in the ammonium- and phosphate-limited near-zero growth cultures, respectively. Glycerol  
197 and succinate were the main contributors, with succinate accounting for 9 % of the  
198 consumed glucose in the ammonium-limited culture.

### 199 **Biomass composition under extreme ammonium and phosphate limitation**

200 To analyse the impact of extreme ammonium and phosphate limitation on biomass  
201 composition, biomass samples from slow growing, steady-state chemostat cultures and from  
202 near-zero growth rate pseudo-steady-state retentostat cultures were analysed for their  
203 elemental and macromolecular compositions (Table 2). In the chemostat cultures as well as  
204 in the retentostat cultures, the content of the growth-limiting element in the biomass was  
205 strongly reduced relative to that of the culture grown under the other nutrient limitation  
206 (Table 2). This difference was even more pronounced in the retentostat cultures than in the  
207 preceding chemostat cultures. The nitrogen content of biomass from ammonium-limited

208 retentostat cultures was ca. 2-fold lower than that of the corresponding phosphate-limited  
209 retentostats, while the phosphorus content of biomass from the phosphate-limited  
210 retentostats was 3.5-fold lower than that of biomass from the ammonium-limited  
211 retentostats. Both in phosphate-limited chemostats and retentostats, a low phosphorus  
212 content was accompanied by a 2-3 fold higher sulfur content than in the corresponding  
213 ammonium-limited cultures. The increased sulfur content in phosphate-limited cultures may  
214 be due to sulfate uptake by high-affinity phosphate transporters (14). Compared with  
215 glucose-limited chemostat cultures of the same *S. cerevisiae* strain at a similar dilution rate  
216 ( $D= 0.022 \text{ h}^{-1}$ , Table 2), the biomass protein content and the total nitrogen content of cells  
217 grown in the ammonium-limited chemostat cultures were over 60 % and 50 % lower,  
218 respectively. Similarly, in the phosphate-limited chemostat cultures, the phosphorus  
219 content of the biomass was ca. 50 % lower.

220 Consistent with their low nitrogen content, ammonium-limited chemostat and retentostat  
221 cultures showed a ca. 2.5-fold lower biomass protein content than the corresponding  
222 phosphate-limited cultures, with the lowest protein content (9.6 %) measured in the  
223 ammonium-limited retentostats (Fig. 2A). Conversely, glycogen contents were higher (5.8  
224 fold in chemostats and 1.8 fold in retentostats) in ammonium-limited cultures than in  
225 phosphate-limited cultures, while trehalose contents were only 30-40 % higher in the  
226 ammonium-limited cultures (Fig. 2B). When analysed throughout the retentostat  
227 experiments, glycogen contents in the ammonium-limited cultures remained consistently  
228 high, while they increased with declining specific growth rate in the phosphate-limited  
229 cultures (Fig. 2C). For both nutrient limitation regimes, the trehalose content reached a  
230 maximum at a specific growth rate of ca.  $0.01 \text{ h}^{-1}$  (Fig. 2D).

## 231 **Metabolic flux analysis**

232 To further investigate the physiological differences between extreme ammonium and  
233 phosphate limitation, metabolic flux analysis was performed for both the slow growing,  
234 steady-state chemostat cultures ( $\mu = 0.025 \text{ h}^{-1}$ ) and near-zero growth, pseudo-steady-state  
235 retentostat cultures ( $\mu < 0.002 \text{ h}^{-1}$ ) (Fig. 3, Supplementary Table S3). At a specific growth  
236 rate of  $0.025 \text{ h}^{-1}$ , fluxes through the glycolysis, tricarboxylic acid cycle (TCA cycle) and  
237 pyruvate branch point were consistently higher in the phosphate-limited cultures than in the  
238 ammonium-limited cultures. This observation indicated a higher contribution of catabolism  
239 in the phosphate-limited cultures. Assuming a P/O ratio of 1 (24), biomass-specific rates of  
240 ATP turnover were ca. 1.3-fold higher in the phosphate-limited chemostat cultures than  
241 in the corresponding ammonium-limited cultures (Fig. 3).

242 In the retentostats, fluxes through the pentose-phosphate pathway (PPP) were extremely  
243 low, which is consistent with the strictly assimilatory role of this central metabolic pathway  
244 in *S. cerevisiae* (25). The glycolytic flux was nearly identical for the two nutrient limitations.  
245 Conversely, distribution of pyruvate over alcoholic fermentation and TCA cycle were  
246 different. Consistent with their lower RQ, phosphate-limited retentostat cultures channeled  
247 a higher fraction of the pyruvate into the TCA cycle than the ammonium limited retentostat  
248 cultures. Estimated non-growth-associated ATP consumption was higher in the phosphate-  
249 limited retentostats ( $3.4 \pm 0.2 \text{ mmol ATP/[g viable biomass]/h}$ ) than in the ammonium-  
250 limited retentostats ( $2.9 \pm 0.1 \text{ mmol ATP/[g viable biomass]/h}$ ) (Fig. 3).

## 251 **Energetics under extreme ammonium and phosphate limitation**

252 Nitrogen and phosphate limitation can both be characterized as non-energy-limited  
253 cultivation regimes. However, because phosphate plays a vital role in cellular energy

254 metabolism and energy status, the intracellular nucleotide levels (ATP, ADP and AMP) and  
255 corresponding adenylate energy charge and ATP/ADP ratios were quantified for both  
256 chemostat and retentostat conditions (Fig. 4). Intracellular levels of all three adenine  
257 nucleotides were consistently higher in the chemostats than in the retentostats. Comparing  
258 these two limitations, both in slow-growth and near-zero growth cultures, intracellular ATP  
259 and AMP levels were consistently lower under phosphate limitation than under ammonium  
260 limitation. In addition, phosphate-limited near-zero growth cultures also showed ca. 40 %  
261 lower ADP levels than the corresponding ammonium-limited cultures, while ADP levels were  
262 identical in phosphate- and ammonium-limited, slow-growing chemostat cultures (Fig. 4A).  
263 Neither the ATP/ADP ratios nor the energy charge in the retentostat cultures differed from  
264 those in the corresponding slow-growing chemostat cultures (Fig. 4B and 4C). However,  
265 ATP/ADP ratios in the phosphate-limited cultures were 30–35 % lower than in the  
266 corresponding ammonium-limited cultures. A similar, less pronounced difference was  
267 observed for the adenylate energy charge. These results show that phosphate limitation  
268 indeed significantly affected cellular energy status.

## 269 **Discussion**

### 270 **Prolonged near-zero growth of *S. cerevisiae* under non-energy-limited conditions**

271 Retentostat cultivation of heterotrophic microorganisms typically involves a constant,  
272 growth-limiting supply rate of the carbon and energy substrate (3). The amount of viable  
273 biomass in such energy-limited retentostats asymptotically increases to a constant value,  
274 while the specific growth rate asymptotically approaches zero. In the resulting pseudo  
275 steady states, biomass-specific substrate supply rates closely match cellular maintenance-  
276 energy requirements (3). The retentostat regimes explored in this study, in which growth

277 was restricted by supply of the nitrogen or phosphorus source, represented a fundamentally  
278 different scenario. While biomass also asymptotically increased to a constant value, the  
279 corresponding constant biomass-specific ammonium or phosphate consumption rates were  
280 not related to maintenance-energy metabolism. Instead, they represented release of  
281 nitrogen- or phosphorus-containing compounds, which were removed via the cell-free  
282 effluent.

283 Excretion of nitrogen- or phosphorus-containing compounds by severely ammonium- or  
284 phosphate-limited yeast cultures appears counter intuitive. Instead, release of these  
285 compounds probably occurs by cell death and/or lysis. *S. cerevisiae* can express a range of  
286 specific and non-specific amino acid permeases (26), while di- and tri-peptides can be  
287 imported by Prt2p (27). Presence of amino acids in culture supernatants is therefore likely to  
288 reflect the kinetics of such transporters, rather than a complete inability for amino-acid  
289 reconsumption by viable cells. Consistent with this hypothesis, extracellular concentrations  
290 of amino acids in the ammonium-limited retentostats were lower than the  $K_m$  values of the  
291 corresponding high-affinity *S. cerevisiae* amino-acid permeases (Supplementary Table S4).  
292 Biomass concentrations in the ammonium- and phosphate-limited retentostats reached  
293 values that were approximately 3-fold higher than the target value of 5 g/L on which design  
294 of growth media and operating conditions were based. This difference could only partially be  
295 attributed to accumulation of non-viable biomass. In addition, strongly reduced contents of  
296 the growth limiting element in the retentostat-grown biomass could explain this large  
297 discrepancy to a large extent.

298 As previously reported for glucose-limited cultures (21), ammonium- and phosphate-limited  
299 cultivation of *S. cerevisiae* at low to near-zero growth rates led to increased intracellular  
300 levels of glycogen and trehalose. This observation confirms that glycogen and trehalose

301 accumulation is a universal physiological response of *S. cerevisiae* at near-zero growth  
302 conditions. Also in faster growing chemostat cultures, nitrogen limitation has been shown to  
303 lead to higher storage carbohydrate levels than other nutrient-limitation regimes (28).  
304 Intracellular reserves of glycogen and trehalose enable survival during carbon and energy  
305 source starvation and can fuel cell cycle progression under carbon- and energy-source  
306 limitation (29). Additionally, upregulation of genes involved in synthesis, metabolism and  
307 degradation of trehalose has been implicated in the extreme heat-shock tolerance of  
308 glucose-limited retentostat cultures of *S. cerevisiae* (6, 30).

### 309 **Energy metabolism of *S. cerevisiae* under extreme ammonium and phosphate** 310 **limitation**

311 Despite strongly reduced phosphate content and low intracellular levels of adenosine  
312 nucleotides, the adenylate energy charge of 0.83 of the phosphate-limited chemostat and  
313 retentostat cultures was within the normal physiological range of 0.7 to 0.95 (31). Also the  
314 adenylate energy charge of 0.88 for the corresponding ammonium-limited cultures indicated  
315 that cells were able to maintain their energy status under extreme nutrient restriction.  
316 Consistent with the well-known tendency of *S. cerevisiae* to exhibit aerobic alcoholic  
317 fermentation when exposed to excess glucose (22), respiratory quotients (RQs) of all  
318 ammonium- and phosphate-limited cultures were above 1. RQ values were lowest at near-  
319 zero growth rates (Supplementary Table S5), indicating that the contribution of fermentative  
320 metabolism decreased with decreasing specific growth rate. Even though *S. cerevisiae* has a  
321 low P/O ratio, respiratory catabolism of glucose yields much more ATP than fermentation  
322 (32). However, its maximum rate of fermentative ATP generation is approximately 2-fold  
323 higher than its maximum rate of respiratory ATP generation (33). These observations

324 underlie a rate/yield trade-off hypothesis, according to which ATP can either be produced  
325 fast (but with a low efficiency) or efficiently (but at a lower maximum rate) (34). The shift  
326 towards a more respiratory metabolism in the near-zero growth rate retentostat cultures is  
327 entirely in line with this hypothesis.

328 Non-growth associated rates of ATP turnover in the aerobic, non-energy-limited cultures  
329 were significantly higher than maintenance-energy requirements estimated from aerobic  
330 and anaerobic energy-limited retentostat studies with the same *S. cerevisiae* strain  
331 (supplementary Fig. S3). While a similar uncoupling of anabolic energy demand and catabolic  
332 energy conservation has been reported for nitrogen-limited chemostat cultures, the  
333 underlying mechanism has not been elucidated (16, 21, 35-38). Quantification of the *in vivo*  
334 cytosolic concentrations of ammonium and ammonia recently showed that, in ammonium-  
335 limited chemostat cultures of *S. cerevisiae* grown at pH 5, cytosolic ammonia concentrations  
336 exceeded extracellular concentrations (39). Diffusion of ammonia from the cells, combined  
337 with reuptake of ammonium cation by the high-affinity uniporter Mep2 (40) and expulsion  
338 of its associated proton by the plasma-membrane H<sup>+</sup>-ATPase Pma1 could lead to a futile  
339 cycle.

340 Extreme phosphate-limited growth of *S. cerevisiae* induces expression of *PHO84*, which  
341 encodes a high-affinity phosphate/proton symporter and vacuolar synthesis of inorganic  
342 polyphosphate(41). By acting as a phosphorus sink, polyphosphate sustains phosphate  
343 uptake at low extracellular concentrations (41, 42). Its synthesis in yeast requires activity of  
344 the vacuolar H<sup>+</sup>-ATPase (V-ATPase) to maintain a proton-motive force across the vacuolar  
345 membrane (41). Although high-affinity phosphate import and subsequent vacuolar  
346 polyphosphate synthesis must have resulted in increased ATP requirements, these are  
347 negligible compared to the observed non-growth associated ATP requirements in the

348 phosphate-limited retentostat cultures. Unless very significant turnover of the  
349 polyphosphate pool has occurred, these additional ATP requirements are likely to have been  
350 caused by other, yet unknown processes.

### 351 **Possible application of severe ammonium or phosphate limitation for industrial** 352 **processes**

353 Metabolic engineering of *S. cerevisiae* has enabled the production of a wide range of  
354 compounds whose biosynthesis from sugars requires a net input of ATP (43). The specific  
355 rate of formation of such ‘anabolic’ products is determined by the capacities and regulation  
356 of the enzymes of the product pathway and connected primary metabolic pathways, as well  
357 as by the continuous (re)generation of cofactors such as NAD(P)H, Coenzyme A and ATP. To  
358 optimize yields of such products, allocation of sugar to growth should be minimized. At the  
359 same time, ATP availability should not limit product formation rates. Theoretically, these  
360 goals can be reconciled by near-zero-growth-rate cultivation under non-energy-limited  
361 conditions. This study shows that, under ammonium limitation as well as under phosphate  
362 limitation, glucose-sufficient, near-zero-growth retentostat cultures of a laboratory strain of  
363 *S. cerevisiae* is able to maintain a normal energy charge and showed only a modest loss of  
364 culture viability. The extremely low protein content of biomass grown in the nitrogen-limited  
365 retentostats is likely to represent a disadvantage for high-level expression of heterologous  
366 product pathways. Moreover, nitrogen limitation is intrinsically poorly suited for production  
367 of proteins and other nitrogen-containing compounds. Extreme phosphate limitation did not  
368 affect biomass protein levels. However, relative to glucose-limited retentostats, both the  
369 ammonium- and phosphate-limited cultures showed increased rates of non-growth  
370 associated ATP dissipation. This increase is undesirable in industrial contexts, as the resulting

371 increased rate of sugar dissimilation would go at the expense of the product yield. Future  
372 research should therefore aim at identifying the causes of non-growth associated ATP  
373 dissipation and on their elimination, either by alternative nutrient limitation regimes, by  
374 strain engineering or by alternative approaches to restrict cell division.

## 375 **Materials and methods**

### 376 **Yeast strain and media**

377 The prototrophic, haploid yeast strain *Saccharomyces cerevisiae* CENPK 113-7D was used in  
378 this study (44). Working stocks were obtained by cultivation in YPD medium (10 g/L Bacto  
379 yeast extract, 20 g/L Bacto peptone and 20 g/L D-glucose). After addition of 30 % (v/v)  
380 glycerol, culture aliquots were stored in sterilized Eppendorf tubes at -80°C.  
381 Ammonium- and phosphate-limited (N- and P-limited) pre-culture and batch culture media  
382 were prepared as described by Boer (16). For N-limited batch cultivation, the medium  
383 contained the following components: 1.0 g of (NH<sub>4</sub>)<sub>2</sub>SO<sub>4</sub>, 5.3 g of K<sub>2</sub>SO<sub>4</sub>, 3.0 g of KH<sub>2</sub>PO<sub>4</sub>, 0.5  
384 g of MgSO<sub>4</sub>·7H<sub>2</sub>O, and 59 g of glucose per liter. For P-limited batch cultivation, the medium  
385 contained 5.0 g of (NH<sub>4</sub>)<sub>2</sub>SO<sub>4</sub>, 1.9 g of K<sub>2</sub>SO<sub>4</sub>, 0.12 g of KH<sub>2</sub>PO<sub>4</sub>, 0.5 g of MgSO<sub>4</sub>·7H<sub>2</sub>O, and 59  
386 g of glucose per liter. In addition, 1 mL/L trace element solution, 1 mL/L vitamin solution  
387 and 0.2 g/L Pluronic 6100 PE antifoaming agent (BASF, Ludwigshafen, Germany) were added.  
388 Trace element and vitamin solutions were prepared as described by Verduyn (45). The  
389 compositions of media for N- and P-limited chemostat cultivation were as described above,  
390 except that the glucose concentration was increased to 120 g/L. For N-limited retentostat  
391 cultivation, the (NH<sub>4</sub>)<sub>2</sub>SO<sub>4</sub> concentration in the medium feed was decreased to 0.1 g/L and  
392 the glucose concentration was 60 g/L. To maintain the same sulfur concentration, the K<sub>2</sub>SO<sub>4</sub>  
393 concentration was increased to 6.46 g/L, the concentrations of the other compounds were

394 the same as in the chemostat medium. For P-limited retentostat cultivation, the  $\text{KH}_2\text{PO}_4$   
395 concentration was lowered to 0.014 g/L and the glucose concentration was 60 g/L.

### 396 **Bioreactor set up**

397 Bench-scale, turbine-stirred 7 L bioreactors (Applikon, Delft, The Netherlands) equipped  
398 with a single six-bladed Rushton turbine impeller with a diameter of 85 mm, were used in  
399 this study. The working volume was controlled at 5 L by placing the bioreactor on an  
400 electronic balance (Mettler Toledo, Columbus, Ohio, USA). During continuous cultivation,  
401 effluent was removed with a peristaltic pump to an effluent vessel, which was placed on an  
402 electronic balance for measurement of the dilution rate ( $D = 0.025 \text{ h}^{-1}$ ). The culture  
403 temperature was maintained at  $30 \pm 0.1^\circ\text{C}$  and the stirrer speed at 500 rpm. Aerobic  
404 conditions were maintained by sparging 0.5 vvm compressed air, controlled by a mass flow  
405 controller (Brooks 5850 TR, Hatfield, PA, USA). The dissolved oxygen concentration was  
406 measured on-line with a DO sensor (Mettler-Toledo GmbH, Greifensee, Switzerland) and  
407 remained above 30 % of air saturation in all experiments. Culture pH was controlled at  $5.00 \pm$   
408  $0.05$  by automated addition of either 2 M KOH or 2 M  $\text{H}_2\text{SO}_4$ , using a Biostat Bplus controller  
409 (Sartorius BBI Systems, Melsungen, Germany). Exhaust gas was cooled to  $4^\circ\text{C}$  by an in-line  
410 condenser and dried by a Nafion dryer (Permapure, Toms River, USA) before entering a  
411 combined paramagnetic/infrared NGA 2000 off-gas analyzer (Rosemount Analytical,  
412 Anaheim, USA) for analysis of  $\text{O}_2$  and  $\text{CO}_2$  concentrations. Off-gas data were acquired with  
413 MFCS/win 3.0 software (Sartorius BBI Systems, Melsungen, Germany).

### 414 **Pre-culture, batch, chemostat and retentostat cultures**

415 Pre-cultures, grown in 500 mL shake flasks containing 200 mL medium, were inoculated with  
416 2 mL of stock culture and grown at  $30^\circ\text{C}$  and at 200 rpm for 8 h in a B Braun Certomat BS-1

417 incubator (Sartorius, Melsungen, Germany ). Bioreactor batch cultures were started by  
 418 transferring 400 mL of preculture to a bioreactor containing 4.6 L of medium. After  
 419 approximately 24 h of batch cultivation, a sharp decrease of the CO<sub>2</sub> concentration in the  
 420 off-gas and a corresponding increase of the dissolved oxygen concentration indicated that  
 421 ammonium or phosphate was depleted. The bioreactors were then switched to chemostat  
 422 cultivation mode and operated at a dilution rate of 0.025 h<sup>-1</sup>. Steady-state was assumed to  
 423 be achieved after 5 volume changes, in which stable (less than 3 % difference over 2 volume  
 424 changes) off-gas CO<sub>2</sub> and O<sub>2</sub> concentrations, culture dry weight and cell counts were  
 425 observed. At that stage, bioreactors were switched from chemostat to retentostat mode by  
 426 redirecting the culture effluent through a filtration probe assembly (Applikon, Delft, The  
 427 Netherlands). Each probe was fitted with a 0.22 μm tubular micro-filtration polypropylene  
 428 membrane (TRACE Analytics, Brunswick, Germany). Because of the limited flow rate capacity  
 429 of each filter, four filtration probes were installed in each bioreactor. Before mounting on  
 430 the filtration probe and autoclaving, membranes were hydrophilized overnight in 70 % (v/v)  
 431 isopropanol.

432 To avoid a sudden decrease of substrate concentrations during the switch from chemostat  
 433 to retentostat mode, a gradual transition from chemostat to retentostat medium was  
 434 accomplished by using two feed pumps. The resulting time-dependent concentrations of  
 435 glucose and of the growth-limiting nutrient ( (NH<sub>4</sub>)<sub>2</sub>SO<sub>4</sub> or KH<sub>2</sub>PO<sub>4</sub>) in the medium are  
 436 described by the following equation:

$$C_s = \frac{e^{(-t/\tau)} * F_{in, ch} * C_{s, ch} + (1 - e^{(-t/\tau)}) * F_{in, re} * C_{s, re}}{e^{(-t/\tau)} * F_{in, ch} + (1 - e^{(-t/\tau)}) * F_{in, re}}$$

437 In this equation, τ is the time constant for the transition which was set to a value of 16.67 h.

438 C<sub>s,ch</sub>, C<sub>s,re</sub>, F<sub>in,ch</sub>, F<sub>in,re</sub> correspond to the nutrient concentrations in the chemostat and

439 retentostat media and the feed rates from the corresponding medium reservoirs,  
440 respectively. Profiles of the resulting concentrations of the limited nutrient and of glucose in  
441 the retentostat feed media during the transition are provided in Supplementary Fig. S3. The  
442 actual medium feed rates during the chemostat and retentostat phases for each experiment  
443 were calculated from the weight increase of the effluent vessels and the addition rates of  
444 base.

#### 445 **Biomass and viability assays**

446 Culture dry weight assays were carried out through a filtration, washing and drying  
447 procedure as described previously (46). Total cell counts were quantified with a Z2 Coulter  
448 counter (50  $\mu\text{m}$  aperture, Beckman, Fullerton, CA). Cell viabilities were determined through  
449 a FungaLight™ Yeast CFDA, AM/Propidium Iodide Vitality Kit ( a cellular membrane integrity  
450 indicator) by flow cytometry and colony-forming-unit counts (6).

#### 451 **Quantification of (by)products and residual substrates**

452 Cell-free effluent samples were harvested from a sample port connected to the retentostat  
453 filters, immediately frozen in liquid nitrogen and stored at  $-80^{\circ}\text{C}$  until analysis. Effluent  
454 concentrations of glucose, ethanol and by-products (glycerol, lactate, acetate, and succinate)  
455 were quantified with HPLC using a Bio-Rad HPX-87H 300 column (7.8 mm). The column was  
456 eluted with phosphoric acid (1.5 mM, 0.6 mL/min ). The detection was performed with a  
457 refractometer ( Walters 2414) and a UV detector (Walters 484, 210 nm). Concentrations of  
458 ammonium and phosphate were quantified with an ammonium cuvette test (0.02-2.5 mg/L  
459  $\text{NH}_4^+$ ) and a phosphate trace cuvette test (0.03-1.5 mg/L  $\text{PO}_4^{3-}$  ), respectively (Hach Lange  
460 GmbH, Düsseldorf, Germany).

## 461 **Balances and rate calculations**

462 Biomass-specific glucose and oxygen consumption rates, and biomass-specific production  
463 rates of ethanol, carbon dioxide and by-products were calculated based on primary  
464 measurements of substrates/products concentration and flow rates in gas and liquid phases.  
465 Data reconciliation was performed as described previously (47). The consistencies of the  
466 thus obtained rates were evaluated by calculation of carbon and degree of reduction  
467 recoveries. Ethanol evaporation via the off-gas of the reactor was quantified as described  
468 previously (48) and was taken into account in calculation of ethanol production rates.  
469 Calculation of specific growth rates and doubling times in retentostat cultures was  
470 performed as described previously (4).

## 471 **Analysis of biomass composition**

472 Around 250 mg of lyophilized biomass was used to determine the elemental (C, H, N, O, P, S)  
473 composition through complete combustion and subsequent gas analysis (carbon dioxide,  
474 water vapour and nitrogen mass fractions), gas chromatography (oxygen) and ICP-MS  
475 (phosphorus and sulphur) (Energy Research Centre, Petten, The Netherlands). Biomass  
476 protein was quantified with the Biuret method as described previously (49). The trehalose  
477 content of the biomass was directly quantified by GC-MS/MS (50) in intracellular metabolite  
478 samples prepared as described below. Glycogen content was quantified through an  
479 enzymatic hydrolysis method (6).

## 480 **Quantification of intracellular metabolites**

481 A rapid sampling device connected to the bioreactor was used to rapidly withdraw broth  
482 samples for intracellular metabolite measurements (51). Approximately 1.2 g broth was  
483 taken and instantaneously quenched in pre-cooled pure methanol (-40°C), followed by a

484 washing procedure with 80 % aqueous methanol (v/v) solution pre-cooled to -40°C.  
485 Metabolite extraction was performed with 75 % (v/v) ethanol (95°C, 3min), followed by  
486 rapid vacuum evaporation until dryness. A detailed protocol has been described previously  
487 (47). Metabolite concentrations were quantified by isotope dilution mass spectrometry (LC-  
488 IDMS/MS and GC-IDMS) using U-<sup>13</sup>C-labeled yeast cell extract as internal standard (52).  
489 Metabolites from glycolysis, TCA cycle and pentose-phosphate pathway as well as amino  
490 acids were quantified according to published protocols (53-55). Intracellular adenine  
491 nucleotide contents (ATP, ADP, AMP) were measured according to (55). The adenylate  
492 Energy Charge(AEC) was calculated as follows:

$$AEC = \frac{ATP + 0.5 * ADP}{ATP + ADP + AMP}$$

### 493 **Metabolic flux analysis**

494 Intracellular flux distributions during steady-state chemostat and pseudo-steady-state  
495 retentostat cultivation were calculated using a slightly modified version of a previously  
496 published stoichiometric model (56), in which the biomass composition was adapted  
497 according to the measurements of the biomass elemental compositions. The input variables  
498 used for the flux analysis are summarized in supplementary Table S3.

### 499 **Acknowledgement**

500 This research was financed by the Netherlands Be-Basic research program (Be-Basic project:  
501 FS10-04 Uncoupling of microbial growth and product formation). We thank Cor Ras, Patricia  
502 van Dam, Silvia Marine and Johan Knoll for analytical support.

### 503 **Reference**

- 504 1. Nielsen J, Keasling JD. 2016. Engineering Cellular Metabolism. Cell 164:1185-1197.
- 505 2. Jansen ML, van Gulik WM. 2014. Towards large scale fermentative production of  
506 succinic acid. Curr Opin Biotechnol 30:190-197.

- 507 3. Ercan O, Bisschops MM, Overkamp W, Jorgensen TR, Ram AF, Smid EJ, Pronk JT,  
508 Kuipers OP, Daran-Lapujade P, Kleerebezem M. 2015. Physiological and  
509 Transcriptional Responses of Different Industrial Microbes at Near-Zero Specific  
510 Growth Rates. *Appl Environ Microbiol* 81:5662-5670.
- 511 4. Boender LG, de Hulster EA, van Maris AJ, Daran-Lapujade PA, Pronk JT. 2009.  
512 Quantitative physiology of *Saccharomyces cerevisiae* at near-zero specific growth  
513 rates. *Appl Environ Microbiol* 75:5607-5614.
- 514 5. Boender LG, van Maris AJ, de Hulster EA, Almering MJ, van der Klei IJ, Veenhuis M, de  
515 Winde JH, Pronk JT, Daran-Lapujade P. 2011. Cellular responses of *Saccharomyces*  
516 *cerevisiae* at near-zero growth rates: transcriptome analysis of anaerobic retentostat  
517 cultures. *FEMS Yeast Res* 11:603-620.
- 518 6. Vos T, Hakkaart XD, de Hulster EA, van Maris AJ, Pronk JT, Daran-Lapujade P. 2016.  
519 Maintenance-energy requirements and robustness of *Saccharomyces cerevisiae* at  
520 aerobic near-zero specific growth rates. *Microb Cell Fact* 15:111.
- 521 7. Bisschops MM, Zwartjens P, Keuter SG, Pronk JT, Daran-Lapujade P. 2014. To divide  
522 or not to divide: a key role of Rim15 in calorie-restricted yeast cultures. *Biochim*  
523 *Biophys Acta* 1843:1020-1030.
- 524 8. Pitt SJ. 1982. Maintenance energy: a general model for energy-limited and energy-  
525 sufficient growth. *Arch Microbiol* 133:300-302.
- 526 9. Brice C, Cubillos FA, Dequin S, Camarasa C, Martinez C. 2018. Adaptability of the  
527 *Saccharomyces cerevisiae* yeasts to wine fermentation conditions relies on their  
528 strong ability to consume nitrogen. *PLoS One* 13:e0192383.
- 529 10. Ibstedt S, Stenberg S, Bages S, Gjuvsland AB, Salinas F, Kourtchenko O, Samy JK,  
530 Blomberg A, Omholt SW, Liti G, Beltran G, Warringer J. 2015. Concerted evolution of  
531 life stage performances signals recent selection on yeast nitrogen use. *Mol Biol Evol*  
532 32:153-161.
- 533 11. Taillandier P, Ramon Portugal F, Fuster A, Strehaiano P. 2007. Effect of ammonium  
534 concentration on alcoholic fermentation kinetics by wine yeasts for high sugar  
535 content. *Food Microbiol* 24:95-100.
- 536 12. Kolouchova I, Matatkova O, Sigler K, Masak J, Rezanka T. 2016. Lipid accumulation by  
537 oleaginous and non-oleaginous yeast strains in nitrogen and phosphate limitation.  
538 *Folia Microbiol (Praha)* 61:431-438.
- 539 13. Gutteridge A, Pir P, Castrillo JI, Charles PD, Lilley KS, Oliver SG. 2010. Nutrient control  
540 of eukaryote cell growth a systems: biology study in yeast. *BMC Biology* 8.
- 541 14. Tai SL, Boer VM, Daran-Lapujade P, Walsh MC, de Winde JH, Daran JM, Pronk JT.  
542 2005. Two-dimensional transcriptome analysis in chemostat cultures. Combinatorial  
543 effects of oxygen availability and macronutrient limitation in *Saccharomyces*  
544 *cerevisiae*. *J Biol Chem* 280:437-447.
- 545 15. Boer VM, Crutchfield CA, Bradley PH, Botstein D, Rabinowitz JD. 2010. Growth-  
546 limiting intracellular metabolites in yeast growing under diverse nutrient limitations.  
547 *Mol Biol Cell* 21:198-211.
- 548 16. Boer VM, de Winde JH, Pronk JT, Piper MD. 2003. The genome-wide transcriptional  
549 responses of *Saccharomyces cerevisiae* grown on glucose in aerobic chemostat  
550 cultures limited for carbon, nitrogen, phosphorus, or sulfur. *J Biol Chem* 278:3265-  
551 3274.

- 552 17. Ramsay A, Douglas L. 1979. Effects of Phosphate Limitation of Growth on the Cel-  
553 Wall and Lipid Composition of *Saccharomyces cerevisiae*. J Gen Microbiol 110:185-  
554 191.
- 555 18. Acquisti C, Kumar S, Elser JJ. 2009. Signatures of nitrogen limitation in the elemental  
556 composition of the proteins involved in the metabolic apparatus. Proc Biol Sci  
557 276:2605-2610.
- 558 19. Wada M, Kato J, Chibata I. 1981. Continuous Production of Ethanol in High  
559 Concentration Using Immobilized Growing Yeast Cells. Appl Microbiol Biotechnol  
560 11:67-71.
- 561 20. Taniguchi M, Wakamiya K, Tsuchiya M, Matsuno R, Kamikubo T. 1983. Continuous  
562 Ethanol Production by Cell-Holding Culture of Yeasts. Appl Microbiol Biotechnol  
563 18:201-206.
- 564 21. Brandberg T, Gustafsson L, Franzén CJ. 2007. The impact of severe nitrogen limitation  
565 and microaerobic conditions on extended continuous cultivations of *Saccharomyces*  
566 *cerevisiae* with cell recirculation. Enzyme Microb Technol 40:585-593.
- 567 22. De Deken BRH. 1966. The Crabtree Effect: A Regulatory System in Yeast. J gen  
568 Microbiol 44:149-156.
- 569 23. Piper PW. 1995. The heat shock and ethanol stress responses of yeast exhibit  
570 extensive similarity and functional overlap. FEMS Microbiol Letters 134:121-127.
- 571 24. Verduyn C, Postma E, Scheffers W, Dijken Jv. 1990. Energetics of *Saccharomyces*  
572 *cerevisiae* in anaerobic glucose-limited chemostat cultures. J Gen Microbiol 136:405-  
573 412.
- 574 25. Steel CC, Grbin PR, Nichol AW. 2001. The pentose phosphate pathway in the yeasts  
575 *Saccharomyces cerevisiae* and *Kloeckera apiculata*, an exercise in comparative  
576 metabolism for food and wine science students. Biochem Mol Biol Educ 29:245-249.
- 577 26. Gournas C, Prévost M, Krammer E-M, André B. 2016. Function and Regulation of  
578 Fungal Amino Acid Transporters: Insights from Predicted Structure, p 69-106. In  
579 Ramos J, Sychrová H, Kschischo M (ed), Yeast Membrane Transport doi:10.1007/978-  
580 3-319-25304-6\_4. Springer International Publishing, Cham.
- 581 27. Melnykov AV. 2016. New mechanisms that regulate *Saccharomyces cerevisiae* short  
582 peptide transporter achieve balanced intracellular amino acid concentrations. Yeast  
583 33:21-31.
- 584 28. Hazelwood LA, Walsh MC, Luttik MA, Daran-Lapujade P, Pronk JT, Daran JM. 2009.  
585 Identity of the growth-limiting nutrient strongly affects storage carbohydrate  
586 accumulation in anaerobic chemostat cultures of *Saccharomyces cerevisiae*. Appl  
587 Environ Microbiol 75:6876-6885.
- 588 29. Silljé HHW, Paalman JWG, Schure EGt, Olsthoorn SQB, Verkleij AJ, Boonstra J, Verrips  
589 CT. 1999. Function of Trehalose and Glycogen in Cell Cycle Progression and cell  
590 viability in *Saccharomyces cerevisiae*. J Bacteriol 181:396-400.
- 591 30. Petitjean M, Teste MA, Francois JM, Parrou JL. 2015. Yeast Tolerance to Various  
592 Stresses Relies on the Trehalose-6P Synthase (Tps1) Protein, Not on Trehalose. J Biol  
593 Chem 290:16177-16190.
- 594 31. De la Fuente IM, Cortes JM, Valero E, Desroches M, Rodrigues S, Malaina I, Martinez  
595 L. 2014. On the dynamics of the adenylate energy system: homeorhesis vs  
596 homeostasis. PLoS One 9:e108676.
- 597 32. Gulik WMv, Heijnen JJ. 1995. A metabolic network stoichiometry analysis of microbial  
598 growth and product formation. Biotechnol Bioeng 48:681-698.

- 599 33. Sonnleitner B, Käppeli O. 1986. Growth of *Saccharomyces cerevisiae* is controlled by  
600 its limited respiratory capacity: Formulation and verification of a hypothesis.  
601 Biotechnol Bioeng 28:927-937.
- 602 34. Pfeiffer T, Schuster S, Bonhoeffer S. 2001. Cooperation and competition in the  
603 evolution of ATP-producing pathways. Science 292:504-507.
- 604 35. Larsson C, Nilsson A, Blomberg A, Gustafsson L. 1997. Glycolytic flux is conditionally  
605 correlated with ATP concentration in *Saccharomyces cerevisiae*: a chemostat study  
606 under Carbon- or Nitrogen-Limiting conditions. J Bacteriol 179:7243-7250.
- 607 36. Varela C, Pizarro F, Agosin E. 2004. Biomass content governs fermentation rate in  
608 nitrogen-deficient wine musts. Appl Environ Microbiol 70:3392-3400.
- 609 37. Larsson C, Stockar Uv, Marison I, Gustafsson L. 1993. Growth and metabolism of  
610 *Saccharomyces cerevisiae* in chemostat cultures under carbon, nitrogen, or carbon  
611 and nitrogen-limiting conditions. J Bacteriol 175:4809-4816.
- 612 38. Lidén G, Persson A, Gustafsson L, Niklasson C. 1995. Energetics and product  
613 formation by *Saccharomyces cerevisiae* grown in anaerobic chemostats under  
614 nitrogen limitation. Appl Microbiol Biotechnol 43:1034-1038.
- 615 39. Cueto-Rojas HF, Milne N, van Helmond W, Pieterse MM, van Maris AJA, Daran JM,  
616 Wahl SA. 2017. Membrane potential independent transport of NH<sub>3</sub> in the absence of  
617 ammonium permeases in *Saccharomyces cerevisiae*. BMC Syst Biol 11:49.
- 618 40. Marini A, Soussi-Boudekou S, Vissers S, Andre B. 1997. A family of ammonium  
619 transporters in *Saccharomyces cerevisiae*. Mol Cell Biol 17:4282-4293.
- 620 41. Ogawa N, DeRisi J, Brown PO. 2000. New Components of a System for Phosphate  
621 Accumulation and Polyphosphate Metabolism in *Saccharomyces cerevisiae* Revealed  
622 by Genomic Expression Analysis. Mol Biol Cell 11:4309-4321.
- 623 42. Gerasimaite R, Mayer A. 2016. Enzymes of yeast polyphosphate metabolism:  
624 structure, enzymology and biological roles. Biochem Soc Trans 44:234-9.
- 625 43. Borodina I, Nielsen J. 2014. Advances in metabolic engineering of yeast  
626 *Saccharomyces cerevisiae* for production of chemicals. Biotechnol J 9:609-20.
- 627 44. Nijkamp JF, Broek Mvd, Datema E, Kok Sd, Bosman L, Luttik MA, Daran-Lapujade P,  
628 Vongsangnak W, Nielsen J, Heijne WH, Klaassen P, Paddon CJ, Platt D, Kötter P, Ham  
629 RCv, Reinders MJ, Pronk JT, Ridder Dd, Daran J-M. 2012. De novo sequencing,  
630 assembly and analysis of the genome of the laboratory strain *Saccharomyces*  
631 *cerevisiae* CEN.PK113-7D, a model for modern industrial biotechnology. Microb Cell  
632 Fact 12.
- 633 45. Verduyn C, Postma E, Scheffers WA, Dijken JPV. 1992. Effect of Benzoic Acid on  
634 Metabolic Fluxes in Yeasts a continuous culture study on the regulation of respiration  
635 and alcoholic fermentation. Yeast 8:501-517.
- 636 46. Postma E, Verduyn C, Scheffers WA, Dijken JPV. 1989. Enzymic analysis of the  
637 crabtree effect in glucose-limited chemostat cultures of *Saccharomyces cerevisiae*.  
638 Appl Environ Microbiol 55:468-477.
- 639 47. Lameiras F, Heijnen JJ, van Gulik WM. 2015. Development of tools for quantitative  
640 intracellular metabolomics of *Aspergillus niger* chemostat cultures. Metabolomics  
641 11:1253-1264.
- 642 48. Cueto-Rojas HF, Maleki Seifar R, Ten Pierick A, Heijnen SJ, Wahl A. 2016. Accurate  
643 Measurement of the in vivo Ammonium Concentration in *Saccharomyces cerevisiae*.  
644 Metabolites 6:1-12.

- 645 49. Lange HC, Heijnen JJ. 2001. Statistical reconciliation of the elemental and molecular  
646 biomass composition of *Saccharomyces cerevisiae*. *Biotechnol Bioeng* 75:334-344.
- 647 50. Niedenfuhr S, ten Pierick A, van Dam PT, Suarez-Mendez CA, Noh K, Wahl SA. 2016.  
648 Natural isotope correction of MS/MS measurements for metabolomics and (13)C  
649 fluxomics. *Biotechnol Bioeng* 113:1137-1147.
- 650 51. Lange HC, Eman M, Zuijlen Gv, Visser D, Dam JCv, Frank J, Mattos MJTd, Heijnen JJ.  
651 2001. Improved rapid sampling for in vivo kinetics of intracellular metabolites in  
652 *Saccharomyces cerevisiae*. *Biotechnol Bioeng* 75:406-415.
- 653 52. Wu L, Mashego MR, van Dam JC, Proell AM, Vinke JL, Ras C, van Winden WA, van  
654 Gulik WM, Heijnen JJ. 2005. Quantitative analysis of the microbial metabolome by  
655 isotope dilution mass spectrometry using uniformly 13C-labeled cell extracts as  
656 internal standards. *Anal Biochem* 336:164-171.
- 657 53. van Dan CJ, Eman RM, Frank J, Lange CH, van Dedem WKG, Heijnen JS. 2002. Analysis  
658 of glycolytic intermediates in *Saccharomyces cerevisiae* using anion exchange  
659 chromatography and electrospray ionization with tandem mass spectrometric  
660 detection. *Analytica Chimica Acta* 460:209-218.
- 661 54. Cipollina C, ten Pierick A, Canelas AB, Seifar RM, van Maris AJ, van Dam JC, Heijnen JJ.  
662 2009. A comprehensive method for the quantification of the non-oxidative pentose  
663 phosphate pathway intermediates in *Saccharomyces cerevisiae* by GC-IDMS. *J*  
664 *Chromatogr B Analyt Technol Biomed Life Sci* 877:3231-3236.
- 665 55. Seifar RM, Ras C, van Dam JC, van Gulik WM, Heijnen JJ, van Winden WA. 2009.  
666 Simultaneous quantification of free nucleotides in complex biological samples using  
667 ion pair reversed phase liquid chromatography isotope dilution tandem mass  
668 spectrometry. *Anal Biochem* 388:213-219.
- 669 56. Daran-Lapujade P, Jansen ML, Daran JM, van Gulik W, de Winde JH, Pronk JT. 2004.  
670 Role of transcriptional regulation in controlling fluxes in central carbon metabolism of  
671 *Saccharomyces cerevisiae*. A chemostat culture study. *J Biol Chem* 279:9125-9138.
- 672

673

674 **Table 1** Physiological parameters of *S. cerevisiae* CEN.PK113-7D cultured in aerobic  
675 ammonium- and phosphate-limited (N- and P-limited) slow growth (SG) ( $\mu = 0.025 \text{ h}^{-1}$ )  
676 steady-state chemostats and near-zero growth (NZG) ( $\mu < 0.002 \text{ h}^{-1}$ ) pseudo-steady-state  
677 retentostats. Data represent averages, with their standard errors, calculated from multiple  
678 measurements obtained from duplicate experiments.

Culture condition	Biomass specific net conversion rates								
	$q_{\text{glucose}}^a$	$q_{\text{ethanol}}$	$q_x$	$q_{\text{glycerol}}$	$q_{\text{succinate}}$	$q_{\text{lactate}}$	$q_{\text{acetate}}$	$q_{\text{O}_2}$	$q_{\text{CO}_2}$
N-limited at SG	14.0 $\pm 0.0$	6.1 $\pm 0.2$	0.96 $\pm 0.09$	0.10 $\pm 0.01$	0.40 $\pm 0.06$	0.070 $\pm 0.001$	0.017 $\pm 0.002$	1.7 $\pm 0.0$	5.5 $\pm 0.2$
P-limited at SG	16.6 $\pm 1.2$	7.9 $\pm 0.3$	0.99 $\pm 0.04$	0.18 $\pm 0.00$	0.15 $\pm 0.01$	0.065 $\pm 0.001$	0.21 $\pm 0.01$	2.1 $\pm 0.0$	6.6 $\pm 0.3$
N-limited at NZG	3.4 $\pm 0.1$	1.5 $\pm 0.0$	--- <sup>b</sup>	0.18 $\pm 0.01$	0.30 $\pm 0.01$	0.048 $\pm 0.002$	0.026 $\pm 0.001$	0.71 $\pm 0.03$	1.5 $\pm 0.0$
P-limited at NZG	3.1 $\pm 0.1$	1.1 $\pm 0.1$	---	0.14 $\pm 0.03$	0.15 $\pm 0.00$	0.000 $\pm 0.000$	0.049 $\pm 0.005$	0.94 $\pm 0.02$	1.6 $\pm 0.1$

Culture condition							Residual nutrient concentrations		
	viability %	RQ <sup>c</sup>	Y <sub>sx</sub> <sup>d</sup>	Y <sub>sp</sub> <sup>e</sup>	carbon recovery %	reduction recovery %	glucose g/L	NH <sub>4</sub> <sup>+</sup> mM	PO <sub>4</sub> <sup>3-</sup> mM
N-limited at SG	93 $\pm 0$	3.1 $\pm 0.0$	0.059 $\pm 0.000$	0.32 $\pm 0.12$	95 $\pm 1$	95 $\pm 1$	16.48 $\pm 0.2$	BD <sup>f</sup>	18.4 $\pm 0.92$
P-limited at SG	91 $\pm 0$	3.1 $\pm 0.1$	0.052 $\pm 0.000$	0.36 $\pm 0.00$	99 $\pm 6$	99 $\pm 3$	18.21 $\pm 0.7$	40.5 $\pm 2.0$	BD
N-limited at NZG	80 $\pm 0$	2.1 $\pm 0.1$	---	0.33 $\pm 0.02$	101 $\pm 2$	98 $\pm 3$	14.99 $\pm 2.01$	BD	18.2 $\pm 0.90$
P-limited at NZG	90 $\pm 0$	1.7 $\pm 0.0$	---	0.28 $\pm 0.03$	98 $\pm 2$	99 $\pm 1$	10.30 $\pm 0.15$	53.5 $\pm 2.7$	BD

679

680

681

682 *a*: Biomass-specific rates were expressed in the unit of  $\text{mCmol/g}_{\text{xv}}/\text{h}$ , and were calculated

683 based on per gram of viable biomass.

684 *b*: Not calculated.

685 *c*: RQ, respiratory quotient ( $q_{\text{CO}_2}/q_{\text{O}_2}$ ).

686 *d*:  $Y_{\text{sx}}$ , Yield of biomass (g biomass/[g glucose consumed]).

687 *e*:  $Y_{\text{sp}}$ , Yield of ethanol (g ethanol/[g glucose consumed]).

688 *f*: BD, below detection limit of assay.

689

690

691

692

693

694

695

696

697

698

699

700

701

702

703

704

705

706

707

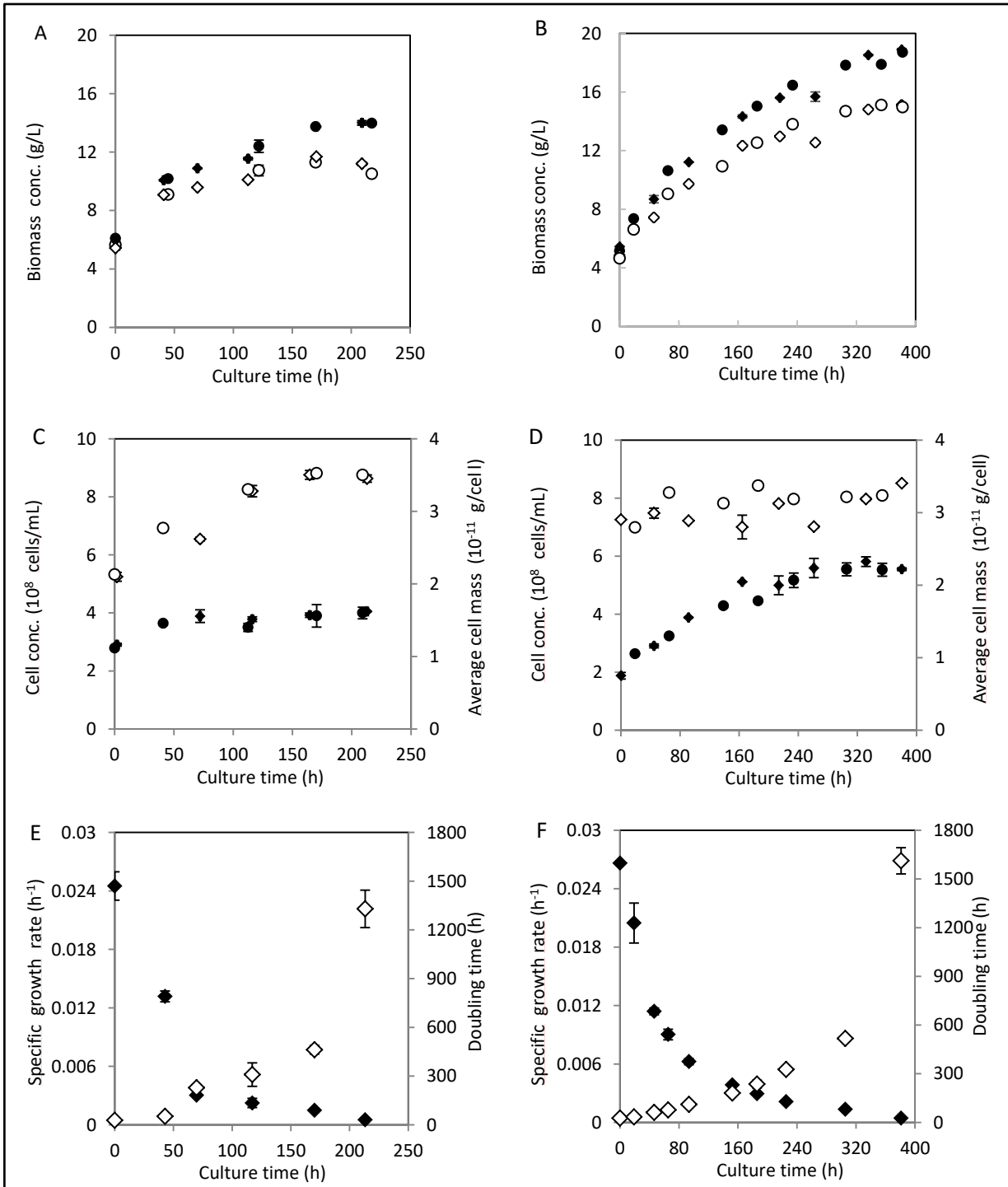
708

709

710 **Table 2** Biomass elemental compositions of *S. cerevisiae* CEN.PK113-7D cultured in aerobic  
711 ammonium- and phosphate-limited (N- and P-limited) slow growth (SG) ( $\mu = 0.025 \text{ h}^{-1}$ )  
712 steady-state chemostats and near-zero growth (NZG) ( $\mu < 0.002 \text{ h}^{-1}$ ) pseudo-steady-state  
713 retentostats. Data represent averages, with standard errors, of measurements from  
714 duplicate cultures and are compared with published values from aerobic glucose-limited (C-  
715 limited) chemostat culture of the same strain (49).

Culture condition	$\mu$ $\text{h}^{-1}$	$f_C$ %	$f_H$ %	$f_N$ %	$f_O$ %	$f_P$ %	$f_S$ %	sum %	C-mol weight g/L
N-limited	0.025	47.0 $\pm 0.0$	7.2 $\pm 0.0$	3.5 $\pm 0.1$	39.5 $\pm 0.4$	1.3 $\pm 0.0$	0.16 $\pm 0.01$	98 $\pm 0$	25.56 $\pm 0.00$
P-limited	0.025	44.0 $\pm 0.2$	7.0 $\pm 0.1$	5.3 $\pm 0.0$	36.9 $\pm 0.3$	0.50 $\pm 0.01$	0.39 $\pm 0.03$	94 $\pm 0$	24.27 $\pm 0.25$
N-limited	< 0.002	49.5 $\pm 0.4$	7.6 $\pm 0.0$	2.5 $\pm 0.0$	39.5 $\pm 1.1$	1.1 $\pm 0.0$	0.11 $\pm 0.01$	100 $\pm 1$	27.33 $\pm 0.22$
P-limited	< 0.002	47.3 $\pm 0.1$	7.2 $\pm 0.0$	4.6 $\pm 0.1$	37.4 $\pm 0.0$	0.29 $\pm 0.00$	0.27 $\pm 0.01$	97 $\pm 0$	25.42 $\pm 0.08$
C-limited	0.022	45.6	6.8	6.6	37.3	1.0	0.22	97	26.4

716  
717  
718  
719  
720  
721  
722  
723  
724  
725  
726  
727  
728  
729  
730



731

732 **Fig. 1** Biomass accumulation, cell counts and specific growth rates in aerobic ammonium-  
 733 and phosphate-limited retentostat cultures of *S. cerevisiae* CEN.PK113-7D. Data of Fig. 1A,  
 734 1B, 1C, and 1D obtained from independent duplicate cultures are shown as circles and  
 735 diamonds, and error bars indicate standard errors of analytical replicates on samples from  
 736 the same culture. Data of Fig. 1C and 1D represent the averages and standard errors of  
 737 measurements on duplicate retentostat cultures.

738 A, B: Total biomass (closed symbols), viable biomass (open symbols) and percentage of  
739 viable biomass in ammonium-limited (A) and phosphate-limited (B) retentostat cultures.  
740 C, D: Cell numbers (closed symbols) and average mass per cell (open symbols) in  
741 ammonium-limited (C) and phosphate-limited (D) retentostat cultures.  
742 E, F: Specific growth rate (closed symbols) and doubling time (open symbols) in ammonium-  
743 limited (E) and phosphate-limited (F) retentostat cultures.

744

745

746

747

748

749

750

751

752

753

754

755

756

757

758

759

760

761

762

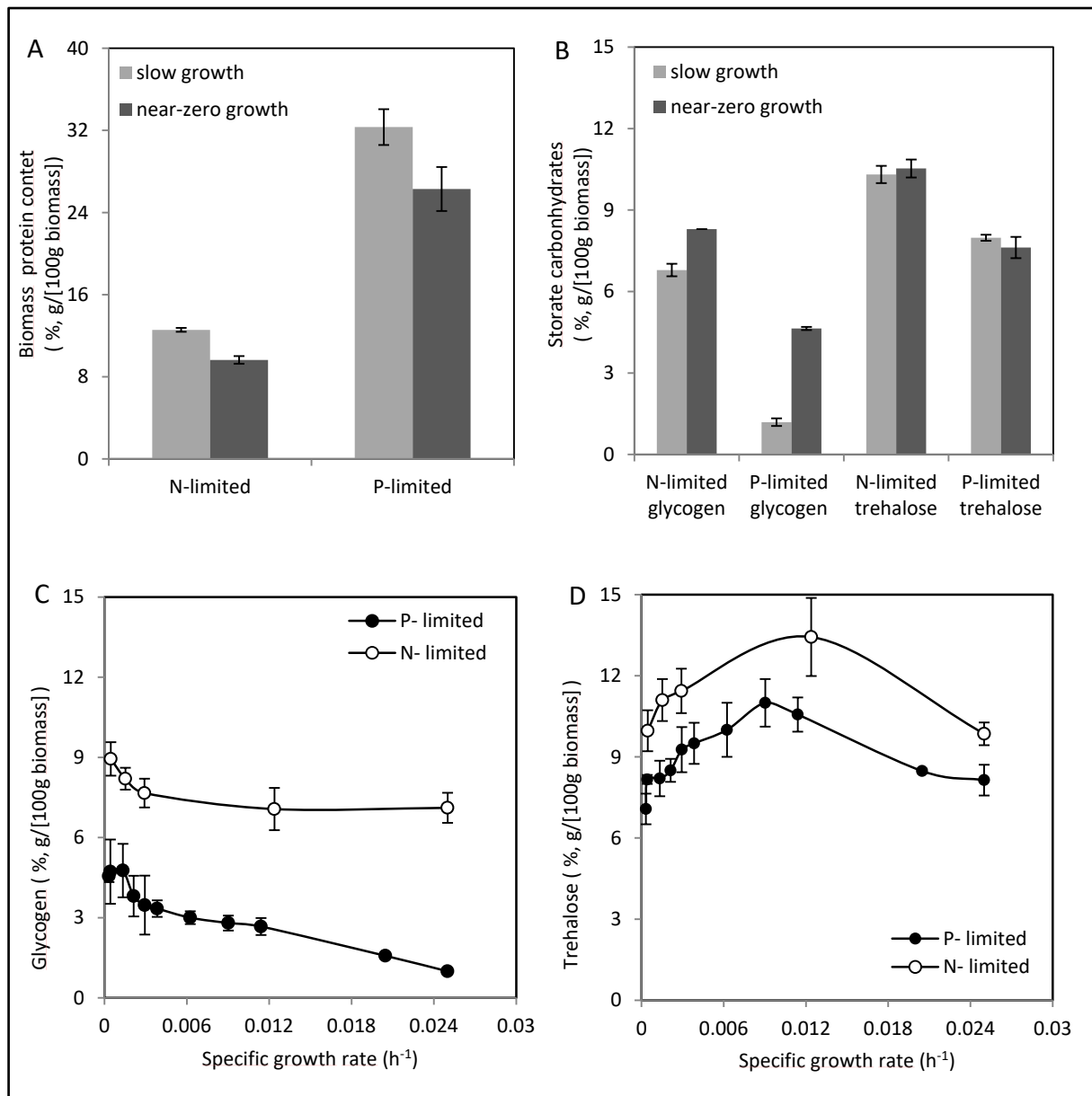
763

764

765

766

767

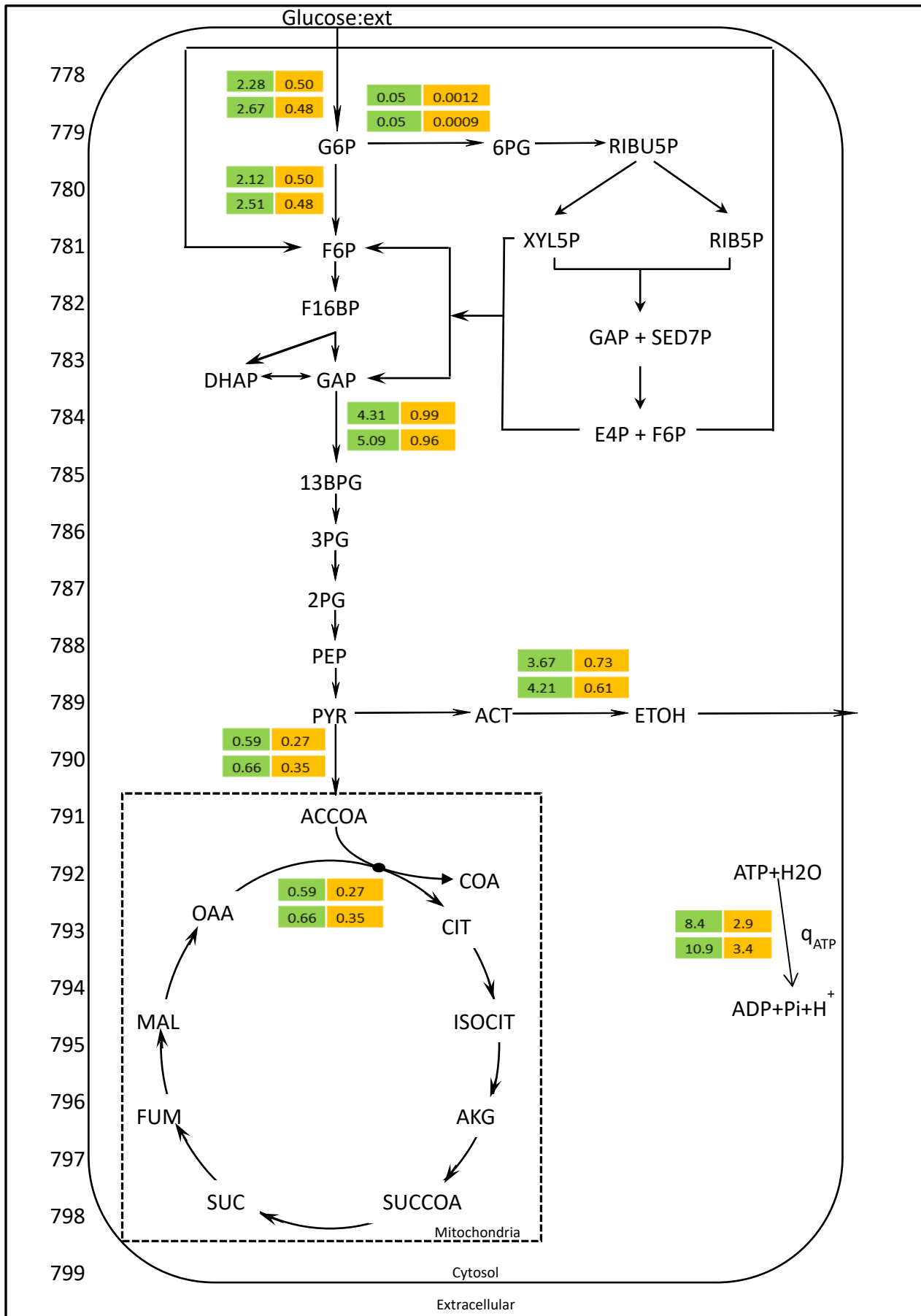


768

769 **Fig. 2** Biomass protein and storage carbohydrates (glycogen and trehalose) contents in  
 770 aerobic ammonium- and phosphate-limited (N- and P-limited) cultures of *S. cerevisiae*  
 771 CEN.PK113-7D. Data represent the averages and standard errors of multiple measurements  
 772 on duplicate cultures.

773 A, B: Biomass protein (A) and storage carbohydrates (glycogen and trehalose) (B). Samples  
 774 were withdrawn from the steady-state, slow growth ( $\mu = 0.025 \text{ h}^{-1}$ ) chemostat cultures, and  
 775 the pseudo-steady-state, near-zero growth ( $\mu < 0.002 \text{ h}^{-1}$ ) retentostat cultures.

776 C, D: Glycogen (C) and trehalose (D) contents vs. the specific growth rate in the prolonged  
 777 retentostat cultures.



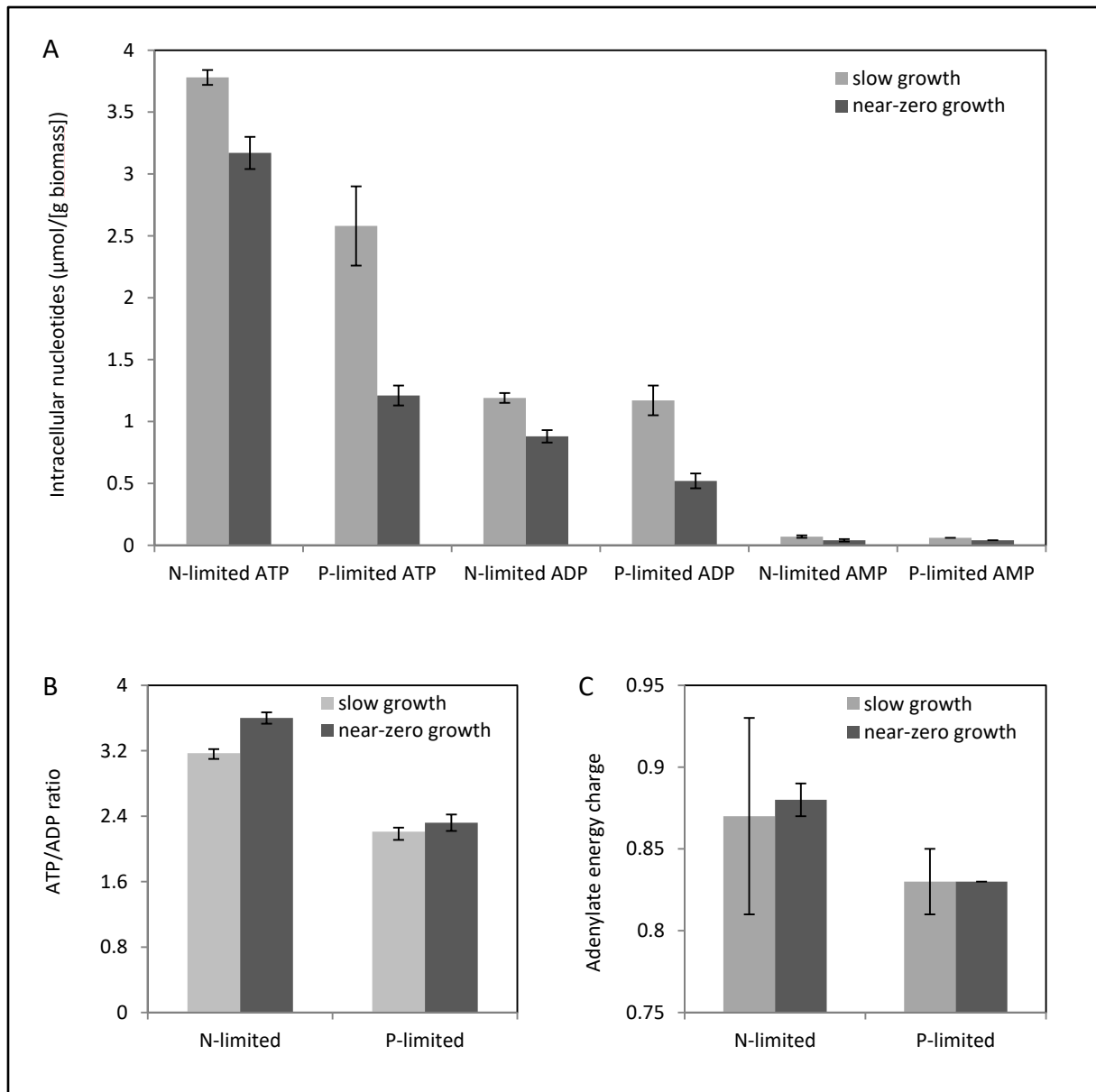
801 **Fig. 3** Metabolic flux analysis in aerobic ammonium- and phosphate-limited (N- and P-  
802 limited) cultures of *S. cerevisiae* CEN.PK113-7D. Flux values present the steady-state, slow  
803 growth (SG) ( $\mu = 0.025 \text{ h}^{-1}$ ) chemostat cultures (numbers on green background), and the  
804 pseudo-steady-state, near-zero growth (NZG) ( $\mu < 0.002 \text{ h}^{-1}$ ) retentostat cultures (numbers  
805 on orange background). Data are expressed in millmoles of per gram viable biomass per  
806 hour and represent the averages of duplicate cultures. Complete flux analysis values and  
807 standard errors were presented in Supplementary Table S3.

808

809

810

811



812

813 **Fig. 4** Intracellular adenosine phosphate concentrations (3A), ATP/ADP ratio (3B) and energy  
 814 charge (3C) in aerobic ammonium- and phosphate-limited (N- and P-limited) cultures of *S.*  
 815 *cerevisiae* CEN.PK113-7D. Data represent the averages and standard errors of multiple  
 816 measurements from duplicate cultures. Samples were withdrawn from the steady-state,  
 817 slow growth ( $\mu = 0.025 \text{ h}^{-1}$ ) chemostat cultures, and the pseudo-steady-state, near-zero  
 818 growth ( $\mu < 0.002 \text{ h}^{-1}$ ) retentostat cultures.

819